^{68}Ga-Fibroblast Activation Protein Inhibitor PET/CT Improves Detection of Intermediate and Low-Grade Sarcomas and Identifies Candidates for Radiopharmaceutical Therapy

Helena Lanzafame[1,2], Ilektra A. Mavroeidi[2,3], Kim M. Pabst[1,2], Mélanie Desaulniers[1,2,4], Marc Ingenwerth[3,5], Nader Hirmas[1,2], Lukas Kessler[1,2,6], Michael Nader[1,2], Timo Bartel[1,2], Stephan Leyser[1,2], Francesco Barbato[1,2], Martin Schuler[2,7], Sebastian Bauer[2,3,7], Jens T. Siveke[2,7,8], Ken Herrmann[1,2,6], Rainer Hamacher*[2,3], and Wolfgang P. Fendler*[1,2]

[1]*Department of Nuclear Medicine, West German Cancer Center, University Hospital Essen, Essen, Germany;* [2]*Cancer Consortium partner site Essen/Düsseldorf, DKFZ and University Hospital Essen, Essen, Germany;* [3]*Department of Medical Oncology, West German Cancer Center, University Hospital Essen, Essen, Germany;* [4]*Department of Nuclear Medicine and Radiobiology, Université de Sherbrooke, Sherbrooke, Québec, Canada;* [5]*Institute of Pathology, University Hospital Essen, Essen, Germany;* [6]*Institute of Diagnostic and Interventional Radiology and Neuroradiology, University Hospital Essen, Essen, Germany;* [7]*National Center for Tumor Diseases West, Campus Essen, Essen, Germany; and* [8]*Bridge Institute of Experimental Tumor Therapy and Division of Solid Tumor Translational Oncology, West German Cancer Center, University Hospital Essen, Essen, Germany*

Fibroblast activation protein-α (FAP) is often highly expressed by sarcoma cells and by sarcoma-associated fibroblasts in the tumor microenvironment. This makes it a promising target for imaging and therapy. The level of FAP expression and the diagnostic value of ^{68}Ga-FAP inhibitor (FAPI) PET for sarcoma subtypes are unknown. We assessed the diagnostic performance and accuracy of ^{68}Ga-FAPI PET in various bone and soft-tissue sarcomas. Potential eligibility for FAP-targeted radiopharmaceutical therapy (FAP-RPT) was evaluated. **Methods:** This prospective observational trial enrolled 200 patients with bone and soft-tissue sarcoma who underwent ^{68}Ga-FAPI PET/CT and ^{18}F-FDG PET/CT (186/200, or 93%) for staging or restaging. The number of lesions detected and the uptake (SUV_{max}) of the primary tumor, lymph nodes, and visceral and bone metastases were analyzed. The Wilcoxon test was used for semiquantitative assessment. The association of ^{68}Ga-FAPI uptake intensity, histopathologic grade, and FAP expression in sarcoma biopsy samples was analyzed using Spearman *r* correlation. The impact of ^{68}Ga-FAPI PET on clinical management was investigated using questionnaires before and after PET/CT. Eligibility for FAP-RPT was defined by an SUV_{max} greater than 10 for all tumor regions. **Results:** ^{68}Ga-FAPI uptake was heterogeneous among sarcoma subtypes. The 3 sarcoma entities with the highest uptake (mean SUV_{max} ± SD) were solitary fibrous tumor (24.7 ± 11.9), undifferentiated pleomorphic sarcoma (18.8 ± 13.1), and leiomyosarcoma (15.2 ± 10.2). Uptake of ^{68}Ga-FAPI versus ^{18}F-FDG was significantly higher in low-grade sarcomas (10.4 ± 8.5 vs. 7.0 ± 4.5, $P = 0.01$) and in potentially malignant intermediate or unpredictable sarcomas without a World Health Organization grade (not applicable [NA]; 22.3 ± 12.5 vs. 8.5 ± 10.0, $P = 0.0004$), including solitary fibrous tumor. The accuracy, as well as the detection rates, of ^{68}Ga-FAPI was higher than that of ^{18}F-FDG in low-grade sarcomas (accuracy, 92.2 vs. 80.0) and NA sarcomas (accuracy, 96.9 vs. 81.9). ^{68}Ga-FAPI uptake and the histopathologic FAP expression score ($n = 89$) were moderately correlated (Spearman $r = 0.43$, $P < 0.0002$). Of 138 patients, 62 (45%) with metastatic sarcoma were eligible for FAP-RPT. **Conclusion:** In patients with low-grade and NA sarcomas, ^{68}Ga-FAPI PET demonstrates uptake, detection rates, and accuracy superior to those of ^{18}F-FDG PET. ^{68}Ga-FAPI PET criteria identified eligibility for FAP-RPT in about half of sarcoma patients.

Key Words: ^{68}Ga-FAPI PET; sarcoma; fibroblast activation protein; theranostic; cancer imaging

J Nucl Med 2024; 65:880–887
DOI: 10.2967/jnumed.123.267248

Sarcomas are rare and heterogeneous tumors that develop from the connective tissue of bone and soft tissue. There are more than 150 subtypes, including low-grade or intermediate or unpredictable tumors without a World Health Organization grade (not applicable [NA]). The outcome for patients with metastatic disease remains poor, with a median overall survival period of approximately 12–18 mo (*1–3*). Fibroblast activation protein-α (FAP) is a type II membrane glycoprotein belonging to the dipeptyl-peptidase family and is present in cancer-associated stromal fibroblasts (*4*,*5*). Cancer-associated stromal fibroblasts constitute an essential component of the tumor microenvironment (*6–8*). With the recent development of radiolabeled FAP inhibitors (FAPIs), these stromal markers have opened up opportunities for molecular imaging and FAP-targeted radiopharmaceutical therapy (FAP-RPT) (*9*). FAPI compounds have been used for the detection of malignant lesions with high stromal content on high-contrast PET/CT images. In recent years, numerous clinical studies have demonstrated high FAPI uptake in various solid tumors, including sarcomas (*10–12*). In addition, for several sarcoma subentities, such as myofibroblastic sarcoma, osteosarcoma, and undifferentiated pleomorphic sarcoma (UPS), histogenesis-specific FAP expression has been reported (*13*). In a previous subgroup analysis, our group proved the high intensity of intratumoral ^{68}Ga-FAPI uptake in sarcoma patients (*14*). Furthermore, we demonstrated a higher detection rate and reproducibility, as well as a more advanced stage of disease, with ^{68}Ga-FAPI PET

Received Dec. 15, 2023; revision accepted Mar. 15, 2024.
For correspondence or reprints, contact Helena Lanzafame (helena.lanzafame@uk-essen.de).
*Contributed equally to this work.
Published online May 9, 2024.

than with ^{18}F-FDG PET (*14*). Accurate staging is of great importance in planning appropriate therapy. In the advanced stage, FAP-RPT has demonstrated signs of efficacy (*15–17*) and is the subject of a prospective phase II safety and tolerability trial in patients with metastatic solid tumors (*18*). FAP-RPT has the potential to improve outcomes for many patients for whom approved therapeutic options are scarce or unfulfilling, including patients with advanced sarcomas. However, sarcoma is a basket term for a broad spectrum of distinct molecular subtypes that show heterogeneous uptake intensity, hence the importance of identifying subentities potentially more suitable for FAP-RPT. To address this issue, we assessed the diagnostic performance and accuracy of ^{68}Ga-FAPI PET versus ^{18}F-FDG PET in a large cohort of sarcoma patients. In addition, we investigated the association between ^{68}Ga-FAPI PET uptake intensity and histopathologic expression of FAP and explored the eligibility of certain sarcoma subentities for FAP-RPT.

MATERIALS AND METHODS

Patient Population

The patient flowchart is illustrated in Figure 1. This is a subgroup analysis of an ongoing ^{68}Ga-FAPI PET observational trial at University Hospital Essen (NCT04571086). Between October 2019 and 2022, ^{68}Ga-FAPI PET was used for the staging or follow-up of sarcomas. In total, 200 bone sarcoma (BS) and soft-tissue sarcoma (STS) patients who underwent ^{68}Ga-FAPI PET were included (31.8% of the cohort). Before enrollment, patients gave written informed consent to undergo ^{68}Ga-FAPI PET for a clinical indication.

Image Acquisition and Evaluation

The synthesis and administration of ^{68}Ga-FAPI-04 (n = 14) and ^{68}Ga-FAPI-46 (n = 186) have been described previously (*9*,*19*). Patients did not require specific preparation before ^{68}Ga-FAPI PET. Clinical PET/CT was performed craniocaudally on 200 patients: 3 (1.5%) with Biograph mMR, 6 (3%) with Biograph mCT, and 191 (95.5%) with Biograph mCT Vision (Siemens Healthineers). The mean activity ± SD injected intravenously was 120 ± 38.3 MBq for ^{68}Ga-FAPI and 248.6 ± 89.2 MBq for ^{18}F-FDG. The mean acquisition time after injection ± SD was 23.5 ± 19.0 min for ^{68}Ga-FAPI PET and 69.5 ± 15.5 min for ^{18}F-^{18}F FDG PET. A diagnostic CT scan was obtained using a standard protocol (80–100 mA, 120 kV) before PET imaging (*20*). For each imaging modality, the number of lesions per region and per patient was recorded. Focal tracer uptake higher than the surrounding background and not associated with physiologic uptake was considered suggestive of malignancy. SUV_{max} was determined for lesions with the highest tracer uptake per region, using Syngo.via software (Siemens Healthineers). All devices had been cross-calibrated to European Association of Nuclear Medicine Research Ltd. accreditation standards. SUV_{mean} was measured in 3 regions normalized according to tumor-to-background ratio (TBR): mediastinal blood pool (center of ascending aorta), liver (unaffected areas of the right lobe), and surrounding normal tissue, including bone or normal soft tissue. The images were read by 2 nuclear medicine physicians or radiologists during a joint reading session. Divergent findings were discussed and resolved by consensus between the readers.

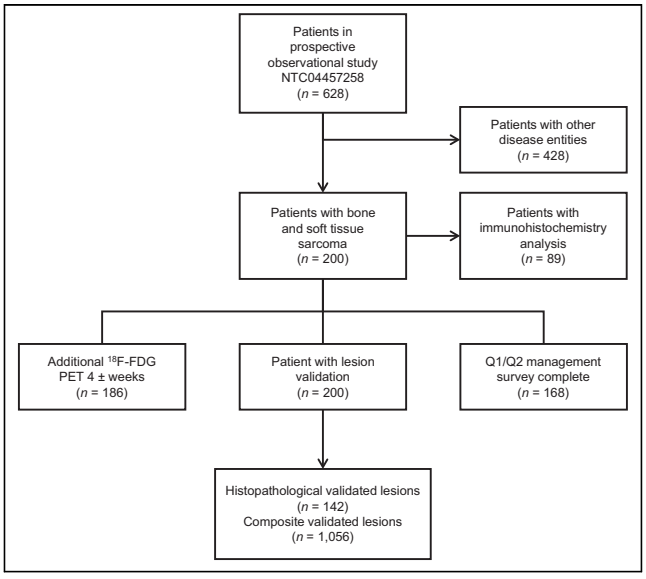

FIGURE 1. Enrollment flowchart. Q = questionnaire.

Lesion Validation

Patients underwent histopathologic analysis of biopsy samples and surgical excision. Lesions that were histopathologically validated within 3 mo of a ^{68}Ga-FAPI PET scan were included in the accuracy analysis. When histopathology was unavailable, validation was performed by correlative or follow-up imaging, that is, CT, MRI, or PET.

Immunohistochemistry

Biopsy and surgical specimens were stained with standard hematoxylin and eosin, as well as FAP immunohistochemistry, and evaluated as previously described (*14*,*21*). FAP expression is categorized semiquantitatively in the histologic section of the tumor as the percentage of FAP-positive cells. Semiquantitative analysis of FAP expression in stroma and tumor cells is assessed using the following scoring system: 0 is the absence or a low degree of FAP-positive cells (<1%), 1+ is FAP-positive in 1%–10% of cells, 2+ is FAP-positive in 11%–50% of cells, and 3+ is FAP-positive in more than 50% of cells. Pathologists were not informed of PET findings.

Management Questionnaires

To assess changes in planned treatment management after ^{68}Ga-FAPI PET, referring physicians completed a questionnaire before PET, which was necessary to assess the patient's existing treatment plan without the contribution of ^{68}Ga-FAPI PET, and a second questionnaire after PET and after reviewing ^{68}Ga-FAPI PET images, which was used to check for implemented change in management.

Statistical Analysis

Descriptive statistics and individual patient data are reported. For continuous data, the mean ± SD SUV_{max} and TBR were compared and tested for statistical differences using Wilcoxon and Mann–Whitney U tests. The sensitivity, specificity, and accuracy of ^{68}Ga-FAPI PET on a per-region basis for the detection of tumor location, confirmed by histopathology or a composite reference standard, were calculated, along with the corresponding 2-sided 95% CIs. A difference of more than 10% was considered relevant. CIs were determined using the Wilson score method. The association of ^{68}Ga-FAPI uptake intensity, grade, and histopathologic FAP expression was analyzed using Spearman r correlation. All statistical analyses were performed using SPSS software (version 20.0; SPSS Inc.) and GraphPad Prism (version 9.1.1; GraphPad Software).

RESULTS

Patient Characteristics

The clinical characteristics of the study population are summarized in Table 1 and Supplemental Table 1 (supplemental materials are available at http://jnm.snmjournals.org). Between October 2020 and 2022, 200 patients were included, 91 (45%) women and 109 (55%) men. Of the 200 patients, 65 (33%) had BS and 135

TABLE 1
Patient Characteristics (n = 200)

Characteristic	Data
Age (y)	55 (39–65)
Sex	
Female	91 (45)
Male	109 (55)
Indication	
Staging	49 (25)
Restaging	151 (75)
BS	65 (33)
Osteosarcoma	17 (9)
Chondrosarcoma	17 (9)
Other BS	15 (7)
Ewing sarcoma	8 (4)
Spindle cell sarcoma	5 (3)
UPS	3 (1)
STS	135 (67)
Other STS	41 (21)
SFT	22 (12)
UPS	15 (7)
Dedifferentiated liposarcoma	15 (7)
Myxoid liposarcoma	14 (6)
Leiomyosarcoma	14 (6)
Synovial sarcoma	7 (4)
Spindle cell sarcoma	7 (4)
Grading	
NA	27 (14)
Low	32 (16)
High	141 (70)

Continuous data are median and interquartile range; qualitative data are number and percentage.

(67%) had STS; 141 (70%) cases were high grade, 32 (16%) cases were low grade, and 27 (14%) cases had no World Health Organization grade (NA). Patients underwent clinical ^{68}Ga-FAPI PET imaging for either staging (49/200 [25%]) or follow-up (151/200 [75%]). Fourteen (7%) patients were imaged with ^{68}Ga-FAPI-04, and 186 (93%) were imaged with ^{68}Ga-FAPI-46. All patients imaged with ^{68}Ga-FAPI-46 underwent ^{18}F-FDG PET imaging within 4 wk. No PET-related adverse events were reported.

FAP Expression in Sarcoma Subtypes

Tumor SUV_{max} and the tumor-to-liver ratio for ^{68}Ga-FAPI versus ^{18}F-FDG in different sarcoma subentities (n = 12) are summarized in Figure 2. We observed heterogeneous tumor uptake of ^{68}Ga-FAPI in our cohort, ranging from an SUV_{max} of 3.1 in myxoid liposarcoma to an SUV_{max} of 47.1 in solitary fibrous tumor (SFT). In terms of mean SUV_{max} ± SD, the 3 sarcoma entities with the highest FAP expression were SFT (24.7 ± 11.9), UPS (18.8 ± 13.1), and leiomyosarcoma (15.2 ± 10.0). By descriptive comparison, the mean SUV_{max} was higher for ^{68}Ga-FAPI than for ^{18}F-FDG in most sarcoma subentities, with the exception of synovial sarcoma, spindle cell sarcoma, and other BS. According to the Wilcoxon test, SUV_{max} and the tumor-to-liver ratio of ^{68}Ga-FAPI PET were significantly higher than those of ^{18}F-FDG PET for SFT (mean SUV_{max} ± SD, 24.7 ± 11.9 vs. 6.8 ± 8.7, P = 0.0005; mean tumor-to-liver ratio ± SD, 22.0 ± 11.9 vs. 4.1 ± 8.9, P = 0.0005) and myxoid liposarcoma (mean SUV_{max} ± SD, 5.6 ± 2.2 vs. 3.5 ± 2.1, P = 0.03; mean tumor-to-liver ratio ± SD, 1.7 ± 1.9 vs. 0.8 ± 1.7, P = 0.04). Additional information on SUVs and TBR is shown in Supplemental Figures 1 and 2 and in Supplemental Table 2.

Based on our previous results (*15*), intense FAP expression, defined by an SUV_{max} of at least 10 in each tumor region, was deemed sufficient for FAP-RPT, as shown in Figure 2A. These PET criteria were met in 62 of 138 (45%) patients with metastatic disease: 16 of 20 with SFT, 3 of 9 with UPS, 7 of 11 with leiomyosarcoma, 5 of 10 with osteosarcoma, 3 of 8 with undifferentiated liposarcoma, 13 of 27 with other STS, 4 of 8 with spindle cell sarcoma, 5 of 13 with chondrosarcoma, 3 of 11 with other BS, 2 of 8 with Ewing sarcoma, and 1 of 4 with synovial sarcoma. FAP expression was highly intense (SUV_{max} of 20 or higher in all regions, as shown in Fig. 2A) in 25 of 138 (18%) patients: 10 of 20 with SFT, 3 of 9 with UPS, 1 of 11 with leiomyosarcoma, 1 of 10 with osteosarcoma, 1 of 8 with undifferentiated liposarcoma, 5 of 27 with other STS, 2 of 8 with spindle cell sarcoma, 1 of 13 with chondrosarcoma, and 1 of 11 with other BS. A complete list of subentities included in the other BS and other STS groups is given in Supplemental Table 3.

^{68}Ga-FAPI versus ^{18}F-FDG uptake was assessed separately for high-grade, NA, and low-grade sarcomas (Fig. 3). Uptake of ^{68}Ga-FAPI versus ^{18}F-FDG was significantly higher in low-grade sarcomas (10.36 ± 8.5 vs. 7.0 ± 4.5, P = 0.01) and NA sarcomas (22.3 ± 12.5 vs. 8.5 ± 10, P = 0.0004), particularly SFT. An example patient is shown in Figure 4.

Detection Efficacy

Detection efficiency is given in Table 2 for primary tumors, lymph nodes, and distant metastases (lung, muscle, viscera [organ], liver, and bone). The detection efficacy of ^{68}Ga-FAPI PET was superior to that of ^{18}F-FDG PET for distant metastases in NA (100% vs. 67%) and low-grade (95% vs. 81%) sarcomas.

Overall, ^{68}Ga-FAPI PET versus ^{18}F-FDG PET detected 1,181 (95%) versus 1,023 (85%) lesions. ^{68}Ga-FAPI PET outperformed ^{18}F-FDG PET in detecting primary tumors (144 [100%] vs. 124 [86%]) and distant metastases (945 [97%] vs. 797 [83%]).

Accuracy

The accuracy of per-region analysis is summarized in Table 3. In total, 142 lesions were histologically validated (110 [77%] primary tumors, 7 [5%] lymph nodes, 22 [15%] visceral metastases, and 3 [2%] bone metastases). In addition, 1,056 lesions were validated by correlative or follow-up imaging (34 [3%] primary tumors, 97 [9%] lymph nodes, 659 [63%] visceral metastases, and 266 [25%] bone metastases). In patients with high-grade sarcomas, sensitivity (96% vs. 94%), specificity (86% vs. 68%), and accuracy (95% vs. 92%) were higher for ^{68}Ga-FAPI than for ^{18}F-FDG. The same was true for patients with NA sarcomas (sensitivity, 96% vs. 83%; specificity, 80% vs. 67%; and accuracy, 95% vs. 82%) and patients with low-grade sarcomas (sensitivity, 93% vs. 85%; specificity, 89% vs. 44%; and accuracy, 92% vs. 80%). Relevant improvement, defined as a difference of 10% or more, was observed with ^{68}Ga-FAPI PET in the specificity of detection of high-grade sarcomas and for all 3 accuracy measures for NA and low-grade sarcomas.

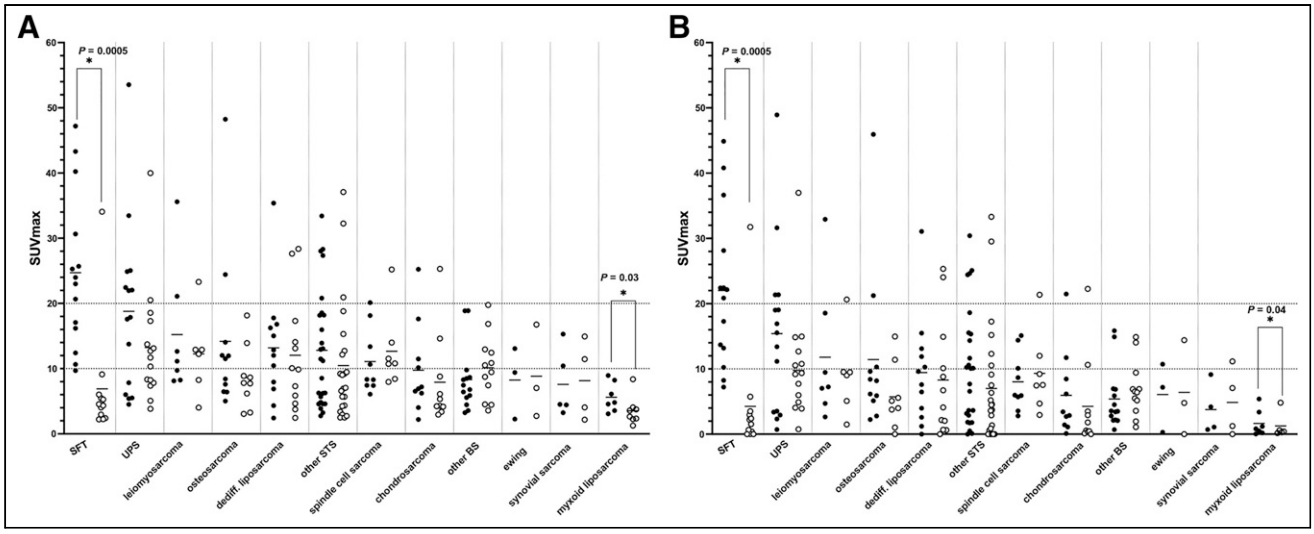

FIGURE 2. Comparison of ^{68}Ga-FAPI and ^{18}F-FDG PET SUV_{max} (A) and tumor-to-liver ratio (B) for sarcoma subentities. Individual data and mean (bars) are shown. Horizontal dotted lines in A indicate patients with SUV_{max} greater than 10 and 20. Black dot = ^{68}Ga-FAPI; white dot = ^{18}F-FDG.

Change in Therapeutic Management

Changes in therapeutic management are presented in Supplemental Table 4. For 168 of 200 (84%) patients, questionnaires completed and returned before and after imaging were available. The management implemented was assessed by reviewing the clinical files. Therapeutic changes based on ^{68}Ga-FAPI PET results were documented in 33 of 168 (20%) patients: 20 (61%) patients changed from active surveillance to chemotherapy, 6 (18%) patients changed from isolated limb perfusion to surgery, 3 (9%) patients changed from a biopsy to surgery, 1 (3%) patient changed from a biopsy to chemotherapy, 1 (3%) patient changed from surgery to chemotherapy, 1 (3%) patient underwent resection plan adjustment, and 1 (3%) patient changed from therapy to active surveillance. Moreover, of the 62 patients with metastatic disease and an SUV_{max} greater than 10, 17 (27%) patients were deemed eligible and underwent at least 1 cycle of FAP-RPT. A patient flowchart is presented in Supplement Figure 3.

PET Versus Immunohistochemistry Target Expression

The association between ^{68}Ga-FAPI PET uptake intensity and FAP immunohistochemistry score is shown in Figure 5 and Supplemental Table 5. Of 89 samples, 30 (34%) samples demonstrated no FAP expression on immunohistochemistry (score 0), and 59 samples had scores 1–3. A moderate positive correlation (Spearman $r = 0.43$, $P = 0.0002$) was found between SUV_{max} and histopathologic FAP expression. Higher uptake values (mean $SUV_{max} \pm SD$) were observed on lesions with FAP score 3 (22.7 ± 14.2) than on those with FAP score 0 (11.4 ± 7.0).

DISCUSSION

In recent years, FAP has been identified as a promising theranostic target for various cancers, including sarcomas (*14*,*15*,*22*,*23*). We analyzed ^{68}Ga-FAPI PET images of 200 patients with 13 subentities of sarcoma. Our study revealed the heterogeneous tumor uptake intensity of FAP, with a mean $SUV_{max} \pm SD$ ranging from 5.6 ± 2.2 in myxoid liposarcoma to 24.7 ± 11.9 in SFT. In addition, we report

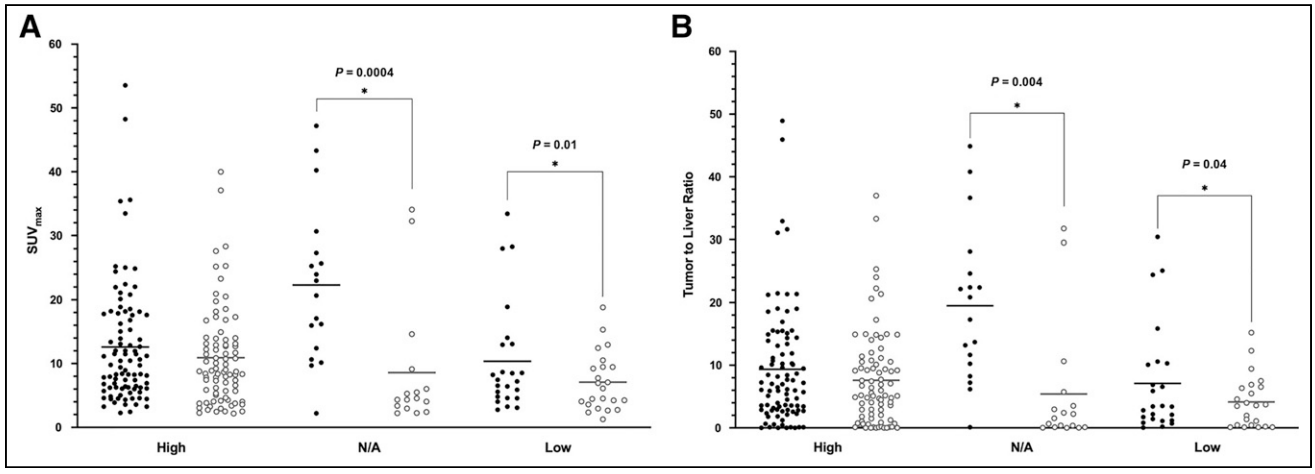

FIGURE 3. Comparison of ^{68}Ga-FAPI and ^{18}F-FDG PET SUV_{max} (A) and tumor-to-liver ratio (B) separated into high-grade, NA, and low-grade groups. Individual data and mean (bars) are shown. Black dot = ^{68}Ga-FAPI; white dot = ^{18}F-FDG.

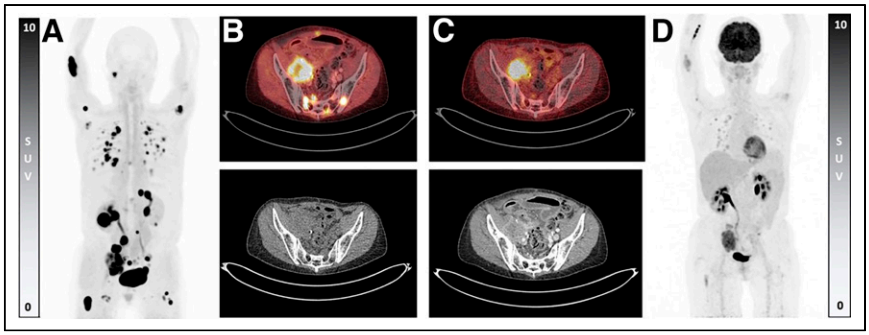

FIGURE 4. 62-y-old patient with metastatic SFT. Higher ^{68}Ga-FAPI uptake (A and B) than ^{18}F-FDG uptake (C and D) is shown in images of primary tumor in right pelvis (SUV_{max} of 25.1 in B vs. 9.0 in C) and multiple pelvic bone metastases (right sacrum, SUV_{max} of 23.0 in B vs. 2.2 in C). Shown are maximum-intensity projection PET images (A and D), axial PET images (B and C, top), and axial CT images (B and C, bottom).

TABLE 2
Detection Efficacy on Per-Region Basis in High-Grade (n = 141), NA (n = 27), and Low-Grade (n = 32) Groups

Lesion	Overall	^{68}Ga-FAPI-46	^{18}F-FDG
High grade			
Primary tumor	100 (100)	100 (100)	84 (84)
Lymph nodes	73 (100)	63 (70)	73 (100)
Distant metastases	563 (100)	563 (100)	524 (93)
Lung	252 (100)	252 (100)	243 (96)
Muscle	52 (100)	52 (100)	49 (94)
Viscera	87 (100)	87 (100)	83 (95)
Liver	32 (100)	32 (100)	28 (88)
Bone	140 (100)	140 (100)	121 (86)
NA			
Primary tumor	17 (100)	17 (100)	15 (88)
Lymph nodes	16 (100)	16 (100)	14 (88)
Distant metastases	286 (100)	286 (100)	191 (67)
Lung	118 (100)	118 (100)	87 (74)
Muscle	25 (100)	25 (100)	14 (56)
Viscera	26 (100)	26 (100)	11 (42)
Liver	12 (100)	12 (100)	8 (67)
Bone	105 (100)	105 (100)	71 (68)
Low grade			
Primary tumor	27 (100)	27 (100)	25 (93)
Lymph nodes	15 (100)	13 (87)	15 (100)
Distant metastases	101 (100)	96 (95)	82 (81)
Lung	31 (100)	31 (100)	22 (71)
Muscle	11 (100)	9 (82)	11 (100)
Viscera	23 (100)	23 (100)	20 (87)
Liver	12 (100)	12 (100)	5 (42)
Bone	24 (100)	21 (88)	24 (100)

Data are number and percentage.

that diagnostic performance of ^{68}Ga-FAPI PET is superior to that of ^{18}F-FDG PET in patients with low-grade and NA sarcomas.

Numerous previous studies have demonstrated the usefulness of ^{18}F-FDG PET imaging for high-grade sarcomas (*24*–*26*). However, sarcomas are highly heterogeneous in terms of aggressiveness and tumor origin. Consequently, imaging these tumors with ^{18}F-FDG PET, as currently indicated for follow-up (*4*,*27*), is often challenging and does not appear to be a viable universal imaging method. In an analysis of 21 tumor entities, Hirmas et al. (*28*) reported that ^{68}Ga-FAPI versus ^{18}F-FDG had higher absolute uptake and TBR, as well as better tumor detection, in sarcomas and pancreatic cancers. Concordant with this observation, we demonstrated that the mean absolute uptake and TBR of ^{68}Ga-FAPI were higher than those of ^{18}F-FDG in all sarcoma subentities except synovial sarcoma, spindle cell sarcoma, and other BS. In a recent prospective study of 45 STS patients, low-grade STS had significantly higher FAP uptake, whereas high-grade STS had significantly higher ^{18}F-FDG uptake (*29*). We also found significantly higher ^{68}Ga-FAPI versus ^{18}F-FDG uptake in low-grade and NA sarcomas. Here, SFT demonstrated high FAP expression, almost twice the average level for all sarcomas. In addition, higher tumor uptake of ^{68}Ga-FAPI translated into a higher per-region detection rate and higher accuracy of ^{68}Ga-FAPI than of ^{18}F-FDG in NA and low-grade sarcomas. ^{68}Ga-FAPI PET led to a change in therapeutic management in around 20% of patients. In around a third of these patients, ^{68}Ga-FAPI PET led from active surveillance to systemic treatment. A small subgroup switched from locoregional to systemic therapy, and a single patient switched from systemic therapy to active surveillance. Most of our cohort were patients with advanced metastatic disease who had already undergone extensive imaging, so ^{68}Ga-FAPI PET only moderately affected clinical decision-making. Nevertheless, we believe that the impact on clinical management will increase if ^{68}Ga-FAPI-PET is performed at earlier stages of the disease. The better tumor detection and specificity of FAPI versus current imaging standards, especially for NA and low-grade sarcomas, could be pivotal to implement staging (i.e., M0 vs. M1) and hence affect therapy planning adjustment (i.e., curative vs. palliative). Moreover, it could implement the assessment of disease extent before local therapies (i.e., target tumor volume before external beam radiotherapy).

Immunohistochemistry analysis was performed on 89 patients. A high level of FAP expression in tumor stroma has been reported previously (*6*,*10*,*30*,*31*). In our study, immunohistochemistry confirmed the presence of the FAP target in tumor lesions and showed a moderate positive correlation, with a higher FAP score associated with higher ^{68}Ga-FAPI PET uptake.

Because of their origin in soft tissue, most sarcomas intrinsically express FAP on the surface of tumor cells and surrounding fibroblasts (*8*,*13*,*32*), which may make this tumor entity particularly suitable for ^{68}Ga-FAPI PET and FAP-RPT (*14*,*28*,*33*,*34*). Metastatic sarcoma has a poor prognosis, with an overall 5-y survival rate of 15% (*35*). Treatment options for this metastatic disease are scarce

TABLE 3
Accuracy of Detection of Sarcoma on Per-Region Basis in High-Grade (n = 141), NA (n = 27), and Low-Grade (n = 32) Groups

Imaging	Sensitivity	Specificity	Accuracy
High grade			
^{68}Ga-FAPI-46	96.4 (93.5–98.3)	85.7 (67.3–95.9)	95.5 (92.5–97.5)
^{18}F-FDG	94.2 (90.8–96.8)	67.9 (47.6–84.2)	91.8 (88.0–94.7)
NA			
^{68}Ga-FAPI-46	95.9 (88.5–99.1)	80.0 (28.4–99.5)	94.9 (87.4–98.6)
^{18}F-FDG	83.3 (72.1–91.4)	66.7 (22.3–95.7)	81.9 (71.1–90.0)
Low grade			
^{68}Ga-FAPI-46	92.6 (83.6–97.6)	88.9 (51.7–99.7)	92.2 (83.8–97.1)
^{18}F-FDG	85.2 (73.8–93.0)	44.4 (13.7–78.8)	80.0 (68.73–88.6)

Data are percentage and 95% CI.

and unfulfilling. FAP-positive cells play a vital role in remodeling the tumor microenvironment. Therefore, FAP is increasingly considered a potential pantumoral target for the design of tumor-targeting drugs, which explains why several in vitro and vivo studies are ongoing.

The development of immunomodulatory therapies based on oncolytic viruses is playing an increasingly important role in the treatment of solid tumors, involving both direct cell lysis and immunogenic cell death. In this context, oncolytic viruses armed with an FAP-targeting bispecific T-cell engager have been designed to target infiltrating lymphocytes toward cancer-associated stromal fibroblasts, thereby enhancing viral propagation and T-cell–mediated cytotoxicity against tumor stroma to improve therapeutic activity (*36*). FAP-targeting bispecific T-cell engager activators, which costimulate T cells and improve tumor cell destruction in FAP-expressing tumors, are the subject of several phase I studies in patients with advanced solid tumors, with preliminary results demonstrating tolerability and safety (*37*,*38*), as well as signs of response (*39*).

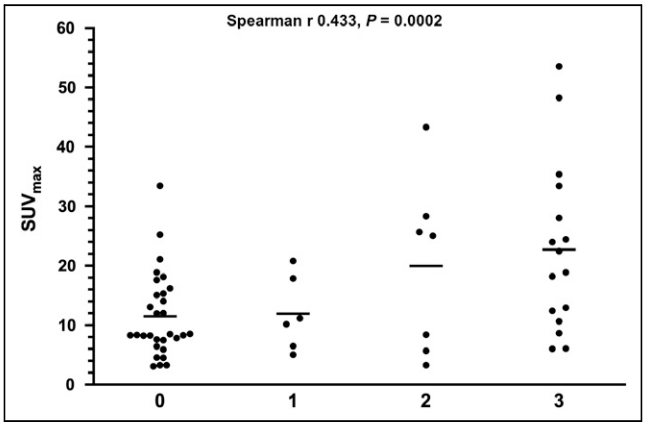

FIGURE 5. Association between ^{68}Ga-FAPI PET uptake intensity (SUV_{max}) and FAP immunohistochemistry score (n = 89). Individual data and mean (bars) are shown. Immunohistochemistry scoring: 0 = no expression (<1%), 1 = 1%–10%, 2 = 11%–49%, + = ≥50% FAP-positive cells. Comparison of SUV_{max} with established immunohistochemistry scoring system showed moderate linear relationship (Spearman r = 0.43, P = 0.0002).

Moreover, when conjugated with doxorubicin, FAP has been used to generate chemotherapeutic prodrugs, activated only in the tumor microenvironment, to selectively release anticancer agents and improve the targeting effect of these cytotoxic agents, thus reducing their systemic side effects (*40*). FAP represents a promising target for other potential treatments, such as immunotherapy (*41*,*42*); FAP-targeted chimeric antigen receptor–T-cell therapy, which is being investigated in 2 phase I clinical trials in patients with malignant pleural mesothelioma (*43*); nectin-4–positive advanced solid malignancies (*44*); and RPT.

RPT is capable of delivering radiation to FAP- and stroma-rich tumor lesions while limiting damage to surrounding tissue. This new therapeutic approach has been widely applied to metastatic neuroendocrine tumors and prostate cancers, improving quality of life and overall survival (*45*,*46*). Several FAP ligands are being investigated in preclinical and clinical settings as theranostic agents. In a head-to-head comparison, ^{177}Lu-labeled FAP ligands were evaluated in vitro in cell lines with low and high human FAP expression and in mice bearing low and high FAP-expressing models. The ^{177}Lu-FAPI-46 dimer presented higher uptake and longer tumor retention than those of the monomer, whereas the tumor–to–critical organ values were in favor of cyclic peptide FAP-2286 (*47*). In a first-in-human dosimetry study, ^{177}Lu-FAP-2286 showed longer tumor retention than a small FAPI tracer, such as FAPI-02/04, and the doses absorbed by the whole body, bone marrow, and kidney were comparable to those of other radiopharmaceuticals previously reported to be effective, namely, ^{177}Lu-DOTATATE and ^{177}Lu-PSMA-617 (*48*). The results of the studies available so far ultimately indicate that dimerization of FAPI small molecules and the cyclic peptide are 2 promising strategies for enhancing the tumor radiation dose.

Various radionuclides are taken into consideration for labeling. If on one side, the β-particle energy of ^{90}Y is higher than that of ^{177}Lu, then on the other side, the longer range of ^{90}Y-β could increase the risk of bone marrow and renal toxicity. Because of the high and precise energy delivery to the tumor per unit of radioactivity, α-emitters, such as ^{225}Ac, could also be potential candidates, as reported in a proof-of-concept study (*49*). FAP-RPT with

^{90}Y-FAPI and ^{177}Lu-FAPI has been documented in several case reports and case series for the treatment of various tumor entities (*17*,*50*–*52*). Our group has previously reported favorable safety and evidence of the efficacy of FAP-RPT in a mixed cohort of patients mainly with metastatic sarcomas (*15*). Furthermore, FAP-RPT is undergoing a prospective phase II safety and tolerability trial in patients with advanced solid tumors (*18*), with preliminary results showing no significant toxicity and some signs of early efficacy (*53*). In accordance with therapeutic criteria (*45*,*54*), intense FAP expression, defined by an SUV_{max} of at least 10 for all tumor lesions, indicated eligibility for FAP-RPT. Based on these criteria, more than half of our patients could be eligible for FAP-RPT. Several subentities of sarcoma, including SFT, UPS, and leiomyosarcoma, demonstrated ^{68}Ga-FAPI uptake that ranged up to highly intense ($SUV_{max} > 20$), indicating favorable target expression for FAP-RPT. Because of the heterogeneous expression of the target, ^{68}Ga-FAPI PET could become a tool for determining eligibility for FAP-RPT and identifying subentities of sarcoma likely to benefit from this therapeutic approach.

Several limitations were identified. We found a moderate correlation between ^{68}Ga-FAPI uptake by PET and target expression by immunohistochemistry. Thus, SUV_{max} may not be representative of the entire tumor lesion, which may underestimate the intralesional heterogeneity of FAP expression. Moreover, some patients did not undergo ^{18}F-FDG PET, potentially leading to a selection bias.

In this analysis, we focus on the diagnostic accuracy of ^{68}Ga-FAPI PET. This study does not include mandatory follow-up. The absence of follow-up data may have led to bias. FAP-RPT eligibility was in line with previously published criteria (*15*). However, these criteria have not yet been validated on the basis of oncologic outcomes.

CONCLUSION

^{68}Ga-FAPI PET demonstrates tumor uptake, detection rate, and accuracy superior to that of ^{18}F-FDG PET in patients with low-grade and NA sarcomas. Tumor uptake for ^{68}Ga-FAPI PET correlated moderately with FAP expression for immunohistochemistry. ^{68}Ga-FAPI PET criteria identified eligibility for FAP-RPT in about half of sarcoma patients, especially those with SFT, UPS, and leiomyosarcoma.

DISCLOSURE

No potential conflict of interest relevant to this article was reported.

KEY POINTS

QUESTION: Does the diagnostic performance of ^{68}Ga-FAPI PET in BS and STS vary according to grade of disease and subentities, and if so, which subentities are more likely to be good candidates for FAP-RPT?

PERTINENT FINDINGS: We observed diagnostic performance and accuracy of ^{68}Ga-FAPI superior to that of ^{18}F-FDG in intermediate and low-grade sarcomas. The subentities that consistently show intense FAPI uptake ($SUV_{max} > 20$), namely, SFT, UPS, and leiomyosarcomas, are more likely to benefit from this therapeutic approach.

IMPLICATIONS FOR PATIENT CARE: ^{68}Ga-FAPI PET is a diagnostic tool for low-grade and NA sarcomas and allows the determination of eligibility for FAP-RPT.

REFERENCES

1. Casali PG, Blay JY, Abecassis N, et al. Gastrointestinal stromal tumours: ESMO–EURACAN–GENTURIS clinical practice guidelines for diagnosis, treatment and follow-up. *Ann Oncol.* 2022;33:20–33.
2. Gronchi A, Miah AB, Dei Tos AP, et al. Soft tissue and visceral sarcomas: ESMO-EURACAN-GENTURIS clinical practice guidelines for diagnosis, treatment and follow-up. *Ann Oncol.* 2021;32:1348–1365.
3. Strauss SJ, Frezza AM, Abecassis N, et al. Bone sarcomas: ESMO–EURACAN–GENTURIS–ERN PaedCan clinical practice guideline for diagnosis, treatment and follow-up. *Ann Oncol.* 2021;32:1520–1536.
4. Classification of Tumours Editorial Board, World Health Organization. *WHO Classification of Tumours.* Vol 3. 5th ed. International Agency for Research on Cancer; 2020.
5. Liu F, Qi L, Liu B, et al. Fibroblast activation protein overexpression and clinical implications in solid tumors: a meta-analysis. *PLoS One.* 2015;10:e0116683.
6. Garin-Chesa P, Old LJ, Rettig WJ. Cell surface glycoprotein of reactive stromal fibroblasts as a potential antibody target in human epithelial cancers. *Proc Natl Acad Sci USA.* 1990;87:7235–7239.
7. Kelly T, Huang Y, Simms AE, Mazur A. Fibroblast activation protein-α: a key modulator of the microenvironment in multiple pathologies. In: Jeon KW, ed. *International Review of Cell and Molecular Biology.* Vol 297. Academic Press; 2012:83–116.
8. Rettig WJ, Garin-Chesa P, Beresford HR, Oettgen HF, Melamed MR, Old LJ. Cell-surface glycoproteins of human sarcomas: differential expression in normal and malignant tissues and cultured cells. *Proc Natl Acad Sci USA.* 1988;85:3110–3114.
9. Lindner T, Loktev A, Altmann A, et al. Development of quinoline-based theranostic ligands for the targeting of fibroblast activation protein. *J Nucl Med.* 2018;59:1415–1422.
10. Altmann A, Haberkorn U, Siveke J. The latest developments in imaging of fibroblast activation protein. *J Nucl Med.* 2021;62:160–167.
11. Ballal S, Yadav MP, Moon ES, et al. Biodistribution, pharmacokinetics, dosimetry of [^{68}Ga]Ga-DOTA.SA.FAPi, and the head-to-head comparison with [^{18}F]F-FDG PET/CT in patients with various cancers. *Eur J Nucl Med Mol Imaging.* 2021;48:1915–1931.
12. Giesel FL, Kratochwil C, Lindner T, et al. ^{68}Ga-FAPI PET/CT: biodistribution and preliminary dosimetry estimate of 2 DOTA-containing FAP-targeting agents in patients with various cancers. *J Nucl Med.* 2019;60:386–392.
13. Dohi O, Ohtani H, Hatori M, et al. Histogenesis-specific expression of fibroblast activation protein and dipeptidylpeptidase-IV in human bone and soft tissue tumours. *Histopathology.* 2009;55:432–440.
14. Kessler L, Ferdinandus J, Hirmas N, et al. ^{68}Ga-FAPI as a diagnostic tool in sarcoma: data from the ^{68}Ga-FAPI PET prospective observational trial. *J Nucl Med.* 2022;63:89–95.
15. Fendler WP, Pabst KM, Kessler L, et al. Safety and efficacy of ^{90}Y-FAPI-46 radioligand therapy in patients with advanced sarcoma and other cancer entities. *Clin Cancer Res.* 2022;28:4346–4353.
16. Ferdinandus J, Fragoso Costa P, Kessler L, et al. Initial clinical experience with ^{90}Y-FAPI-46 radioligand therapy for advanced-stage solid tumors: a case series of 9 patients. *J Nucl Med.* 2022;63:727–734.
17. Baum RP, Schuchardt C, Singh A, et al. Feasibility, biodistribution, and preliminary dosimetry in peptide-targeted radionuclide therapy of diverse adenocarcinomas using ^{177}Lu-FAP-2286: first-in-humans results. *J Nucl Med.* 2022;63:415–423.
18. A study of ^{177}Lu-FAP-2286 in advanced solid tumors (LuMIERE). ClinicalTrials.gov website. https://clinicaltrials.gov/study/NCT04939610. Updated February 6, 2024. Accessed April 9, 2024.
19. Nader M, Valla DF, Vriamont C, et al. [^{68}Ga]/[^{90}Y]FAPI-46: automated production and analytical validation of a theranostic pair. *Nucl Med Biol.* 2022;110–111:37–44.
20. Boellaard R, Delgado-Bolton R, Oyen WJG, et al. FDG PET/CT: EANM procedure guidelines for tumour imaging—version 2.0. *Eur J Nucl Med Mol Imaging.* 2015;42:328–354.
21. Henry LR, Lee H-O, Lee JS, et al. Clinical implications of fibroblast activation protein in patients with colon cancer. *Clin Cancer Res.* 2007;13:1736–1741.
22. Giesel FL, Kratochwil C, Schlittenhardt J, et al. Head-to-head intra-individual comparison of biodistribution and tumor uptake of ^{68}Ga-FAPI and ^{18}F-FDG PET/CT in cancer patients. *Eur J Nucl Med Mol Imaging.* 2021;48:4377–4385.
23. Hamacher R, Lanzafame H, Mavroeidi IA, et al. Fibroblast activation protein inhibitor theranostics: the case for use in sarcoma . *PET Clin.* 2023;18:361–367.
24. Charest M, Hickeson M, Lisbona R, Novales-Diaz J-A, Derbekyan V, Turcotte RE. FDG PET/CT imaging in primary osseous and soft tissue sarcomas: a retrospective review of 212 cases. *Eur J Nucl Med Mol Imaging.* 2009;36:1944–1951.

25. Lim HJ, Johnny Ong C-A, Tan JW-S, Ching Teo MC. Utility of positron emission tomography/computed tomography (PET/CT) imaging in the evaluation of sarcomas: a systematic review. *Crit Rev Oncol Hematol.* 2019;143:1–13.
26. Macpherson RE, Pratap S, Tyrrell H, et al. Retrospective audit of 957 consecutive ^{18}F-FDG PET-CT scans compared to CT and MRI in 493 patients with different histological subtypes of bone and soft tissue sarcoma. *Clin Sarcoma Res.* 2018;8:9.
27. Strauss SJ, Frezza AM, Abecassis N, et al. Bone sarcomas: ESMO-EURACAN-GENTURIS-ERN PaedCan clinical practice guideline for diagnosis, treatment and follow-up. *Ann Oncol.* 2021;32:1520–1536.
28. Hirmas N, Hamacher R, Sraieb M, et al. Fibroblast-activation protein PET and histopathology in a single-center database of 324 patients and 21 tumor entities. *J Nucl Med.* 2023;64:711–716.
29. Gu B, Liu X, Wang S, et al. Head-to-head evaluation of [^{18}F]FDG and [^{68}Ga]Ga-DOTA-FAPI-04 PET/CT in recurrent soft tissue sarcoma. *Eur J Nucl Med Mol Imaging.* 2022;49:2889–2901.
30. Liu F, Qi L, Liu B, et al. Fibroblast activation protein overexpression and clinical implications in solid tumors: a meta-analysis. *PLoS One.* 2015;10:e0116683.
31. Sgouros G, Bodei L, McDevitt MR, Nedrow JR. Radiopharmaceutical therapy in cancer: clinical advances and challenges. *Nat Rev Drug Discov.* 2020;19:589–608.
32. Dolznig H, Schweifer N, Puri C, et al. Characterization of cancer stroma markers: in silico analysis of an mRNA expression database for fibroblast activation protein and endosialin. *Cancer Immun.* 2005;5:10.
33. Kratochwil C, Flechsig P, Lindner T, et al. ^{68}Ga-FAPI PET/CT: tracer uptake in 28 different kinds of cancer. *J Nucl Med.* 2019;60:801–805.
34. Koerber SA, Finck R, Dendl K, et al. Novel FAP ligands enable improved imaging contrast in sarcoma patients due to FAPI-PET/CT. *Eur J Nucl Med Mol Imaging.* 2021;48:3918–3924.
35. Survival rates for soft tissue sarcoma. American Cancer Society website. https://www.cancer.org/cancer/types/soft-tissue-sarcoma/detection-diagnosis-staging/survival-rates.html. Updated February 2, 2021. Accessed April 9, 2024.
36. de Sostoa J, Fajardo CA, Moreno R, Ramos MD, Farrera-Sal M, Alemany R. Targeting the tumor stroma with an oncolytic adenovirus secreting a fibroblast activation protein-targeted bispecific T-cell engager. *J Immunother Cancer.* 2019;7:19.
37. Simon G, Subbiah V, Rosen L, et al. First-in-human phase 1a study of NG-641, a tumour-selective vector expressing a FAP-TAc bispecific antibody and immune enhancer module, in patients with metastatic/advanced epithelial tumours (STAR) [abstract]. *J Immunother Cancer.* 2022;10:762.
38. Gomez-Roca CA, Steeghs N, Gort EH, et al. Phase I study of MP0317, a FAP-dependent DARPin, for tumor-localized CD40 activation in patients with advanced solid tumors [abstract]. *J Clin Oncol.* 2023;41:2584.
39. Melero I, Tanos T, Bustamante M, et al. A first-in-human study of the fibroblast activation protein–targeted, 4-1BB agonist RO7122290 in patients with advanced solid tumors. *Sci Transl Med.* 2023;15:eabp9229.
40. McLaughlin F, Poplawski SE, Sanford DG, et al. AVA6000, a novel precision medicine, targeted to the tumor microenvironment via fibroblast activation protein (FAP) mediated cleavage [abstract]. *Cancer Res.* 2022;82:1815.
41. Lee IK, Noguera-Ortega E, Xiao Z, et al. Monitoring therapeutic response to anti-FAP CAR T cells using [^{18}F]AlF-FAPI-74. *Clin Cancer Res.* 2022;28:5330–5342.
42. Bughda R, Dimou P, D'Souza RR, Klampatsa A. Fibroblast activation protein (FAP)-targeted CAR-T cells: launching an attack on tumor stroma. *ImmunoTargets Ther.* 2021;10:313–323.
43. Hiltbrunner S, Britschgi C, Schuberth P, et al. Local delivery of CAR T cells targeting fibroblast activation protein is safe in patients with pleural mesothelioma: first report of FAPME, a phase I clinical trial. *Ann Oncol.* 2021;32:120–121.
44. Interventional therapy sequential with the fourth-generation CAR-T targeting nectin4/FAP for malignant solid tumors. ClinicalTrials.gov website. https://clinicaltrials.gov/study/NCT03932565. Updated November 18, 2020. Accessed April 9, 2024.
45. Strosberg JR, Caplin ME, Kunz PL, et al. ^{177}Lu-DOTATATE plus long-acting octreotide versus high-dose long-acting octreotide in patients with midgut neuroendocrine tumours (NETTER-1): final overall survival and long-term safety results from an open-label, randomised, controlled, phase 3 trial. *Lancet Oncol.* 2021;22:1752–1763.
46. Sartor O, Hope TA, Calais J, Fendler WP. Oliver Sartor talks with Thomas A. Hope, Jeremie Calais, and Wolfgang P. Fendler about FDA approval of PSMA. *J Nucl Med.* 2021;62:146–148.
47. Millul J, Koepke L, Haridas GR, Sparrer KMJ, Mansi R, Fani M. Head-to-head comparison of different classes of FAP radioligands designed to increase tumor residence time: monomer, dimer, albumin binders, and small molecules vs peptides. *Eur J Nucl Med Mol Imaging.* 2023;50:3050–3061.
48. Baum RP, Schuchardt C, Singh A, et al. Feasibility, biodistribution, and preliminary dosimetry in peptide-targeted radionuclide therapy of diverse adenocarcinomas using ^{177}Lu-FAP-2286: first-in-humans results. *J Nucl Med.* 2022;63:415–423.
49. Watabe T, Liu Y, Kaneda-Nakashima K, et al. Theranostics targeting fibroblast activation protein in the tumor stroma: ^{64}Cu- and ^{225}Ac-labeled FAPI-04 in pancreatic cancer xenograft mouse models. *J Nucl Med.* 2020;61:563.
50. Assadi M, Rekabpour SJ, Jafari E, et al. Feasibility and therapeutic potential of ^{177}Lu-fibroblast activation protein inhibitor-46 for patients with relapsed or refractory cancers: a preliminary study. *Clin Nucl Med.* 2021;46:e523–e530.
51. Ballal S, Yadav MP, Kramer V, et al. A theranostic approach of [^{68}Ga]Ga-DOTA.SA.FAPi PET/CT-guided [^{177}Lu]Lu-DOTA.SA.FAPi radionuclide therapy in an end-stage breast cancer patient: new frontier in targeted radionuclide therapy. *Eur J Nucl Med Mol Imaging.* 2021;48:942–944.
52. Kaghazchi F, Aghdam RA, Haghighi S, Vali R, Adinehpour Z. ^{177}Lu-FAPI therapy in a patient with end-stage metastatic pancreatic adenocarcinoma. *Clin Nucl Med.* 2022;47:e243–e245.
53. McConathy J, Dhawan M, Goenka A, et al. ^{177}Lu-FAP-2286 in patients with advanced or metastatic solid tumors: initial data from a phase 1/2 study investigating safety, pharmacokinetics, dosimetry, and preliminary antitumor activity (LuMIERE) [abstract]. *J Nucl Med.* 2022;63:2271.
54. Sartor O, de Bono J, Chi KN, et al. Lutetium-177–PSMA-617 for metastatic castration-resistant prostate cancer. *N Engl J Med.* 2021;385:1091–1103.